Studies of Distortional Isomers. 2. Evidence That Green $[LWOCl_2]PF_6$ Is a Ternary Mixture

Patrick J. Desrochers,[1a] Kenneth W. Nebesny,[1a] Michael J. LaBarre,[1a] Michael A. Bruck,[1a] George F. Neilson,[1b] R. P. Sperline,[1a] John H. Enemark,*[,1a] Gabriele Backes,[1c] and Karl Wieghardt[1d]

Departments of Chemistry and Materials Science and Engineering, University of Arizona, Tucson, Arizona 85721, Department of Chemical and Biological Sciences, Oregon Graduate Institute of Science and Technology, Beaverton, Oregon 97006-1999, and Lehrstuhl für Anorganische Chemie I, Ruhr-Universität, D-4630 Bochum, Germany

Received September 23, 1993®

Studies of the "green isomer of $[LWOCl_2]PF_6$" (L = 1,4,7-trimethyl-1,4,7-triazacyclononane) have revealed that this material is not a distortional isomer of blue $[LWOCl_2]PF_6$ but rather is a ternary mixture of blue $[LWOCl_2]PF_6$, a tungsten(IV)–oxo species, and a tungsten(VI)–dioxo species characterized by a *cis*-WO_2^{2+} unit. Tungsten 4f X-ray photoelectron spectroscopy (XPS) has shown the green material prepared according to literature methods to be a variable mixture of these three tungsten oxidation states. Blue $[LWOCl_2]PF_6$ is implicated as the single paramagnetic tungsten(V) component in the green material. Identical EPR spectra were recorded for frozen solutions of blue $[LWOCl_2]PF_6$ and of the supposed green isomer, showing a rhombic d^1 system ($g_1 = 1.869$, $g_2 = 1.811$, $g_3 = 1.761$; $A_1 = 57.4 \times 10^{-4}$ cm^{-1}, ^{183}W). Broad resonances due to blue $[LWOCl_2]PF_6$ were observed in the proton NMR spectrum of the green material. Visible spectra of the green material revealed two absorptions at 419 and 695 nm, consistent with those reported previously; however, the relative intensities of these peaks were found to vary with reaction time, indicating the composite nature of the green material. Visible spectroscopy also confirmed the rhombic system for blue $[LWOCl_2]PF_6$, whose broad peak previously reported at 715 nm was resolved into two overlapping peaks centered at 722 and 618 nm, respectively. Infrared analyses of the mixed green material characterized the tungsten(VI) component as a *cis*-WO_2^{2+} species from a pair of distinct peaks at 960 and 923 cm^{-1}. The relative intensity of these and the ν(W=O) peak of blue $[LWOCl_2]PF_6$ (981 ± 2 cm^{-1}; confirmed with ^{18}O substitution by IR and Raman) varied with reaction time. Cyclic voltammetry of the green material revealed several solvent-dependent waves consistent with its multicomponent character and solvent-dependent equilibria involving the components in solution. Column chromatography separated some of the blue $[LWOCl_2]PF_6$ from the green material, but additional chromatography yielded no further separation of the remaining green mixture. Competitive solution equilibria are invoked to explain this unusual chromatographic behavior. These combined results refute the existence of distortional isomerism in $[LWOCl_2]PF_6$, one of the most widely cited examples of this phenomenon in transition-metal complexes.

Introduction

In 1985 the isolation and X-ray structural characterization of blue and green forms of $[LWOCl_2]PF_6$ (L = 1,4,7-trimethyl-1,4,7-triazacyclononane) were reported.[2] The green form was unusual in that the apparent W=O distance (1.89(2) Å) was unexpectedly long compared to that in the blue form (1.72(2) Å) and compared to similar distances in other oxo compounds of tungsten and molybdenum.[2a] The different W=O distances for the blue and green forms of $[LWOCl_2]PF_6$ were reminiscent of the blue and green forms of *cis,mer*-$MoOCl_2(PMe_2Ph)_3$ reported in 1971.[3] Indeed, the properties of the blue and green forms of $[LWOCl_2]PF_6$ seemed to substantiate the original proposed by Chatt *et al.* of a "new type of isomerism,"[3] denoted as "distortional isomerism".[3,4]

Our collaborative investigation of the blue and green forms of $[LWOCl_2]PF_6$ described herein was initially stimulated by a desire to better understand the spectroscopic properties of the two forms and to determine the kinetic and thermodynamic factors for interconverting "distortional isomers". Further stimulus was provided by the papers of Yves, Lledos, Burdett, and Hoffmann[5] that provided a theoretical framework for the existence of "distortional" (bond stretch) isomers in coordination compounds.[6]

Concurrently, some of us were also reinvestigating the blue and green *cis,mer*-$MoOCl_2(PMe_2Ph)_3$ system originally reported by Chatt *et al.*[3] In 1991, three different research groups published independent structural,[7] theoretical,[8] and spectroscopic[7,9] evidence conclusively demonstrating that the green form of *cis,mer*-$MoOCl_2(PMe_2Ph)_3$ was actually a subtle mixture of blue *cis,mer*-$MoOCl_2(PMe_2Ph)_3$[10] and yellow *mer*-$MoCl_3(PMe_2Ph)_3$. These results called into question the entire concept of distortional (bond stretch) isomers in coordination compounds.[11-14] The recent

• Abstract published in *Advance ACS Abstracts*, December 1, 1993.

(1) (a) Department of Chemistry, University of Arizona. (b) Department of Materials Science and Engineering, University of Arizona. (c) Oregon Graduate Institute of Science and Technology. (d) Ruhr-Universität.

(2) (a) Backes-Dahmann, G.; Wieghardt, K.; Nuber, B.; Weiss, J. *Angew. Chem., Int. Ed. Engl.* **1985**, *24*, 777. (b) Backes-Dahmann, G.; Wieghardt, K. *Inorg. Chem.* **1985**, *24*, 4049.

(3) Chatt, J.; Manojlović-Muir, L.; Muir, K. W. *Chem. Commun.* **1971**, 655.

(4) Butcher, A. V.; Chatt, J. *J. Chem. Soc. A* **1970**, 2652.

(5) (a) Yves, J.; Lledos, A.; Burdett, J. K.; Hoffmann, R. *J. Am. Chem. Soc.* **1988**, *110*, 4506. (b) Yves, J.; Lledos, A.; Burdett, J. K.; Hoffmann, R. *J. Chem. Soc., Chem. Commun.* **1988**, 140.

(6) The terms "distortional isomerism" and "bond stretch isomerism" are often used interchangeably. For a discussion of the differences between these two similar concepts see: Bashall, A. P.; Bligh, S. W. A.; Edwards, A. J.; Gibson, V. C.; McPartlin, M.; Robinson, O. B. *Angew. Chem., Int. Ed. Engl.* **1992**, *31*, 1607.

(7) (a) Yoon, K.; Parkin, G.; Rheingold, A. L. *J. Am. Chem. Soc.* **1992**, *114*, 2210. (b) Yoon, K.; Parkin, G.; Rheingold, A. L. *J. Am. Chem. Soc.* **1991**, *113*, 1437.

(8) Song, J.; Hall, M. B. *Inorg. Chem.* **1991**, *30*, 4433.

(9) Desrochers, P. J.; Nebesny, K. W.; LaBarre, M. J.; Lincoln, S. E.; Loehr, T. M.; Enemark, J. H. *J. Am. Chem. Soc.* **1991**, *113*, 9193.

(10) Blue *cis,mer*-$MoOCl_2(PMe_2Ph)_3$ can exist in C_s and C_1 forms in the solid state that exhibit different conformations of the phosphine groups.[7a] Recently, Bashall *et al.*[6] identified the conditions required to crystallize each form and clearly demonstrated that the two forms have significantly different P–Mo–Cl and P–Mo–P angles but nearly identical normal Mo=O distances of 1.663(2) Å (C_s) and 1.682(7) Å (C_1); ν(Mo=O) for the two forms are 955 cm^{-1} (C_s) and 943 cm^{-1} (C_1).

(11) Gibson, V. C.; McPartlin, M. *J. Chem. Soc., Dalton Trans.* **1992**, 947.

(12) Mayer, J. M. *Angew. Chem., Int. Ed. Engl.* **1992**, *31*, 286.

0020-1669/94/1333-0015$04.50/0

demonstration that $LTiOCl_2$ and $LTiCl_3$ form subtle mixtures that behave as apparently homogeneous substances[15] provided additional impetus to reinvestigate the blue and green forms of $[LWOCl_2]PF_6$ by a variety of physical and spectroscopic methods. Here we provide evidence that the green form is actually a *ternary* mixture of oxo–W(IV,V,VI) complexes that are in dynamic equilibrium in solution.

Experimental Section

Synthesis. Tungsten hexacarbonyl and sodium hexafluorophosphate were obtained from Aldrich Chemicals; 1,4,7-trimethyl-1,4,7-triazacyclononane (L) was prepared as previously described[16] or obtained from Aldrich Chemicals and used as received. Concentrated DCl/D_2O was obtained from Aldrich Chemicals. Chemical analyses were performed by Atlantic Microlabs, Norcross, GA.

Blue and Green $[LWOCl_2]PF_6$. The crude blue and green forms were prepared according to the original procedures.[2] Two different green samples were isolated as a result of running the reaction between $LW(CO)_3$ and 10 M HCl for 2 days (2-day green) and 7 days (7-day green), respectively. Each was purified by column chromatography (*vide infra*) prior to subsequent characterizations. In the synthesis of the blue form, a gray solid was separated from the reaction mixture by decantation prior to the addition of solid sodium hexafluorophosphate to the clear blue decantate.

The synthesis of blue $[W^{18}OCl_2]PF_6$ was carried out in a nitrogen-filled glovebag. To 60 mg of maroon $[LWCl_3]Cl$[2b] was added 0.5 mL of $H_2{}^{18}O$ (95% ^{18}O) in a small test tube. The mixture was stirred magnetically, its color changed immediately from maroon to green-blue, and then a gray-blue slurry appeared. After being stirred for 1 h, the mixture was centrifuged, and the resultant clear blue supernatant was decanted. To this decantate was added about 80 mg of solid $NaPF_6$; dissolution of the sodium salt initiated the immediate precipitation of $[LW^{18}OCl_2]PF_6$ as a pale blue solid. Infrared analysis: $\nu(W{=}{}^{18}O)$ at 925 cm^{-1}; other features identical to those of $[LW^{16}OCl_2]PF_6$.

Chromatography. Acidic alumina (Aldrich Chemicals, 58 Å, 150 mesh) columns were prepared from a slurry of the alumina in the initial eluent of 65:35 (v/v) chloroform/acetonitrile. All samples were loaded onto their respective columns using a concentrated acetonitrile solution of the crude material. The crude blue form was purified by passage down a 6 × 2 cm column using the 65:35 chloroform/acetonitrile eluent at a flow rate of ca. 1 mL/min. The material precipitated by the addition of aqueous sodium hexafluorophosphate in the synthesis of the green form was partially isolated by passing it down a 25 × 2 cm column. Initially an eluent of 65:35 chloroform/acetonitrile was used at a flow rate of ca. 1 mL/min. As many as four, but more typically three, distinct bands were eventually visible. The leading bands were yellow unreacted $LW(CO)_3$ (when present) and $[LW(CO)_3Cl]PF_6$, followed by a blue band and a trailing yellow-green band. By the time the blue band was approximately two-thirds of the way down the column, visible separation was achieved between it and the trailing yellow-green band. After complete elution of the blue fraction, the eluent was changed to neat acetonitrile to facilitate the final elution of the yellow-green fraction.

Electrochemistry. Cyclic voltammograms of dissolved samples (ca. 1 mM) were recorded at 100 mV/s in DMF (unless otherwise noted) that had been stored over 4-Å molecular sieves. Tetrabutylammonium tetrafluoroborate (100 mM) was used as supporting electrolyte. Platinum disk working, platinum pin auxiliary, and standard calomel reference electrodes were used in conjunction with an IBM EC/225 voltammetric analyzer. Potentials were referenced relative to the ferrocene/ferrocenium redox couple as an internal standard.

Infrared Spectroscopy. Infrared spectra were recorded as KBr pellets on a Perkin-Elmer Model 1800 FTIR using DTGS detection. Spectra were transferred from Perkin-Elmer format to MS-DOS (tm) format via an RS-232 interface for manipulation.[17] Spectra were fitted with Gaussian peak shapes using Peakfit 3.10 (Jandel Scientific, 2591 Kerner Blvd., San Rafael, CA 94901). For the ^{18}O-exchange experiments aliquots of an acetonitrile solution were spotted onto a NaCl plate and the solvent was allowed to evaporate. Too few data points were available to allow curve fitting of the isotopically exchanged spectra.

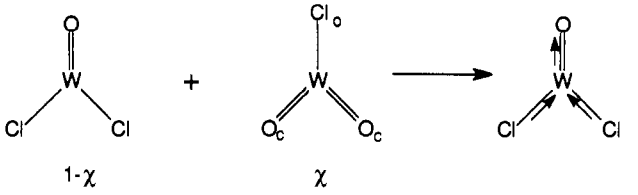

Figure 1. Model for compositional disorder calculations of the $WOCl_2$ and $W(O_c)_2Cl_o$ fragments showing the effects on the apparent W–O and W–Cl distances in $WOCl_2$ (cf. Figure 14). χ = mole fraction of $W(O_c)_2Cl_o$.

Raman Spectroscopy. Instrumental details are described elsewhere.[9] Spectra were recorded using 514.5-nm-excitation radiation for samples packed in glass capillaries.

Proton NMR Spectroscopy. Spectra were recorded on a Bruker AM 500-MHz spectrometer at the ambient probe temperature of 22 °C using a block size of 16 or 32 kbytes. A 30° pulse width was used for spectra where the diamagnetic resonances were of interest (scan width 6000–7000 Hz), and 90° pulse width was used for broad scans (50 000 Hz) of samples where the paramagnetic resonances were of interest. Pure samples were run in deuterioacetonitrile (as received). Each spectrum was internally referenced relative to residual CH_3CN protons at 1.93 ppm.

Electron Paramagnetic Resonance Spectroscopy. Spectra were recorded on a Bruker ESP 300E spectrometer. Samples were measured in quartz tubes submersed in a Dewar flask of liquid nitrogen fitted to the spectrometer cavity.

UV–Visible Electron Spectroscopy. All spectra were recorded at ambient temperature on a Cary 14 spectrometer equipped with an On-Line Instrument Systems (OLIS) data acquisition system using quartz cells (1.0-cm path length).

X-ray Photoelectron Spectroscopy. Instrumental details are described elsewhere.[18] Mg Kα (100 W) radiation was used on solid samples pressed into indium foil. The binding energies are referenced relative to the carbon 1s peak at 284.6 eV to correct for differences due to charging effects within individual samples. No detectable degradation of the samples was observed over the course of the measurements run at ambient temperature.

X-ray Crystallography. Single-crystal X-ray diffraction data were collected on an Enraf-Nonius CAD4 κ-axis diffractometer using graphite-monochromated Mo Kα radiation (supplementary material). Empirical absorption corrections based on a series of ψ scans were applied to the data. Powder diffraction data were recorded on an automated Scintag θ–θ powder diffractometer using Cu Kα (computer-converted to Cu Kα_1) radiation patterns of solid samples spread uniformly over a glass slide. Reflections were recorded over a range of 2θ ($5 \leq 2\theta \leq 70°$) in approximately 30 min. Scintag software was used in the subsequent data reductions and unit cell refinements derived from these powder data.

The effects of compositional disorder of $WOCl_2$ and WO_2Cl units on the apparent W=O and W—Cl distances were modeled by using a modified version of the program NICSYN[19] in conjunction with existing SDP software.[20] Positions for the W atoms of the two fragments were made coincident. The O and Cl positions for the $WOCl_2$ fragment were taken from the structure of blue $[LWOCl_2]PF_6$;[2a] the O_c and Cl_o positions of the WO_2Cl fragment were calculated to lie along the W–Cl and W–O vectors of the $WOCl_2$ fragment, respectively (Figure 1). The multiplicities of the appropriate atoms were varied as a function of the compositional disorder of the two fragments, and the calculated structure factors ($0 \leq 2\theta \leq 50°$) for these simple disordered models were then used as the hypothetical observed data for a standard least-squares refinement of the structure of a single, ordered $WOCl_2$ fragment.[21]

(13) Parkin, G. *Acc. Chem. Res.* **1992**, *25*, 455.
(14) Parkin, G. *Chem. Rev.* **1993**, *93*, 887.
(15) Bodner, A.; Jeske, P.; Weyhermüller, T.; Wieghardt, K.; Dubler, E.; Schmalle, H.; Nuber, B. *Inorg. Chem.* **1992**, *31*, 3737.
(16) Wieghardt, K.; Chaudhuri, P.; Nuber, B.; Weiss, J. *Inorg. Chem.* **1982**, *21*, 3086.
(17) Sperline, R. P. *Appl. Spectrosc.* **1991**, *45*, 1046–1047.
(18) Ingram, J. C.; Nebesny, K. W.; Pemberton, J. E. *Appl. Surf. Sci.* **1990**, *44*, 279.
(19) B. A. Frenz & Associates, Inc., College Station, TX 77840, and Enraf-Nonius, Delft, Holland.
(20) Frenz, B. A. The Enraf-Nonius CAD 4 SDP-A Real-time System for Concurrent X-ray Data Collection and Crystal Structure Determination. In *Computing in Crystallography*; Schenk, H., Olthof-Hazelkamp, R., vanKonigsveld, H., Bassi, G. C., Eds.; Delft University Press: Delft, Holland, 1978; pp 64–71.
(21) Desrochers, P. J. Ph.D. Dissertation, University of Arizona, 1992.

Results and Discussion

Synthesis. The blue form of $[LWOCl_2]PF_6$ is reproducibly synthesized by the published procedure involving the reaction of $[LWCl_3]Cl$ with water.[2] The physical properties of the compound, including the single-crystal structure (*vide infra*), are identical to those originally reported.[2]

The original synthesis of the green form involved refluxing $LW(CO)_3$ in 10 M HCl for 2 days (reaction 1),

$$LW(CO)_3 + 10\ M\ HCl \rightarrow \text{green "}[LWOCl_2]^+\text{"} \quad (1)$$

followed by precipitation by the addition of aqueous sodium hexafluorophosphate to the reaction mixture.[2] In the present study the course of reaction 1 over time has been monitored by three different spectroscopic methods (IR, EPR, NMR).

Addition of sodium hexafluorophosphate to an aliquot of the reaction mixture precipitates all cationic species as PF_6^- salts. An infrared spectrum of the PF_6^- precipitate obtained early in the reaction (within 30 min) shows that a considerable amount of the starting material has been oxidized to the known seven-coordinate W(II) complex $[LW(CO)_3Cl]^+$, which contains three ν(CO) peaks that are distinct from those in the W(0) starting material, $LW(CO)_3$. Indeed, this same reaction scheme is the reported method for preparing $[LW(CO)_3Cl]PF_6$ after 2 h.[2] These characteristic ν(CO) peaks persist in the infrared spectra of all PF_6^- salts isolated from reaction 1, even after several days, and appreciably diminish in intensity only after about 4 days. Over time, peaks assignable to $\nu(W^{V}{=}O)$ of $[LWOCl_2]^+$ and the $\nu(W^{VI}{=}O)$ bands characteristic of a *cis*-WO_2^{2+} unit can eventually be observed in aliquots taken from reaction 1. Several species may be present in the green material precipitated upon addition of PF_6^- to the reaction mixture after 2 days, but every spectroscopic and chromatographic characterization of the green material isolated from reaction 1 indicates that blue $[LWOCl_2]PF_6$ is one of the components (*vide infra*).

Chromatography has proven to be a powerful method for demonstrating that the materials originally formulated as distortional isomers are actually mixtures. The simple separation of green $MoOCl_2(PMe_2Ph)_3$ by thin-layer chromatography was the first reported case of chromatographic analysis of any material believed to be a distortional isomer.[9]

Three key characteristics of the green product of reaction 1 are illustrated by passing this material down an acidic alumina column. First, the crude green material isolated from the reaction between $LW(CO)_3$ and 10 M HCl is a multicomponent mixture that separates into $[LW(CO)_3Cl]PF_6$, a blue band, and a yellow-green band, respectively, in order of elution. Second, the blue band is visibly separated from the trailing yellow-green band on the column, and this isolable blue fraction is pure $[LWOCl_2]PF_6$. Third, NMR and EPR spectroscopies (*vide infra*) confirm the presence of blue $[LWOCl_2]^+$ in the trailing yellow-green band (Figures 2 and 3), *but re-elution of this trailing fraction under identical conditions returns the green material unchanged with no further separation.* This unusual chromatographic behavior of the products of reaction 1 has significant ramifications for understanding the true character of the apparently homogeneous green material (*vide infra*) believed to be the green "distortional isomer"[2a] of $[LWOCl_2]PF_6$.

500-MHz proton NMR confirms the presence of blue $[LWO_2Cl]PF_6$ in the apparently homogeneous green fraction. Scans of both blue $[LWOCl_2]PF_6$ and the green material over a large spectral bandwidth reveal up to six resonances due to blue $[LWO_2Cl]PF_6$ in each spectrum in the region from −20 to +40 ppm (Figure 2). Proton NMR was used to follow the course of Reaction 1 by carrying out the reaction in concentrated DCl/D_2O and periodically recording the NMR spectrum. The initial proton spectrum was dominated by resonances assignable to the diamagnetic species $LW(CO)_3$ and $[LW(CO)_3Cl]^+$. These resonances decayed with time and were replaced by broad resonances characteristic of blue $[LWOCl_2]^+$. The concentration of diamagnetic species appeared to be at a minimum after about 45 h. With increasing reaction time, new diamagnetic species appeared. It was not possible to absolutely assign the proton resonances in these spectra due to the changing acid concentration in successive aliquots as reaction 1 progressed.

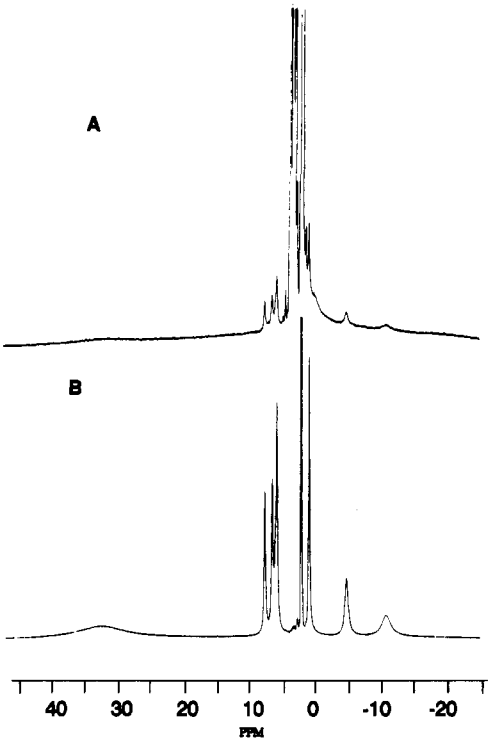

Figure 2. 500-MHz proton NMR spectra of green "$[LWOCl_2]PF_6$" (A) and blue $[LWOCl_2]PF_6$ (B).

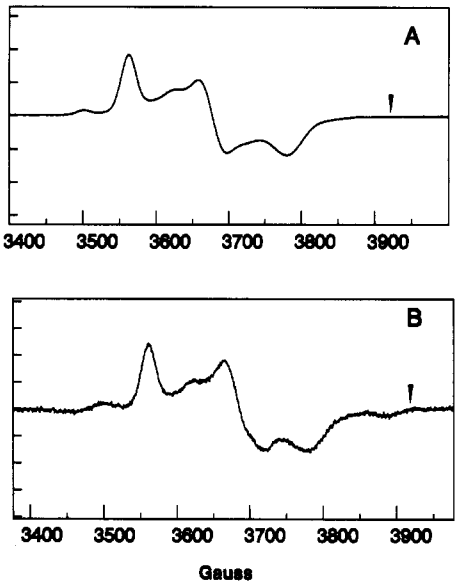

Figure 3. EPR spectra of blue $[LWOCl_2]PF_6$ (A) and green "$[LWOCl_2]PF_6$" (B) in acetonitrile/toluene glasses at 77 K. Wedge: $g = 1.700$. The EPR parameters for (A) are $g_1 = 1.896$, $g_2 = 1.811$, $g_3 = 1.761$, $A_1 = 57.4 \times 10^{-4}$ cm^{-1}; the g values for (B) are within experimental error (±0.003) of those for (A).

Electron paramagnetic resonance (EPR) spectra of the blue and green forms in toluene/acetonitrile glasses at 77 K (Figure 3) are nearly identical. The highest g value shows hyperfine splitting due to coupling of the single unpaired electron with the ^{183}W nucleus ($I = {}^1/_2$, natural abundance = 14.4%); spectral simulation confirmed this assignment. An original sample of the green form[2] gave an identical EPR spectrum when recorded on

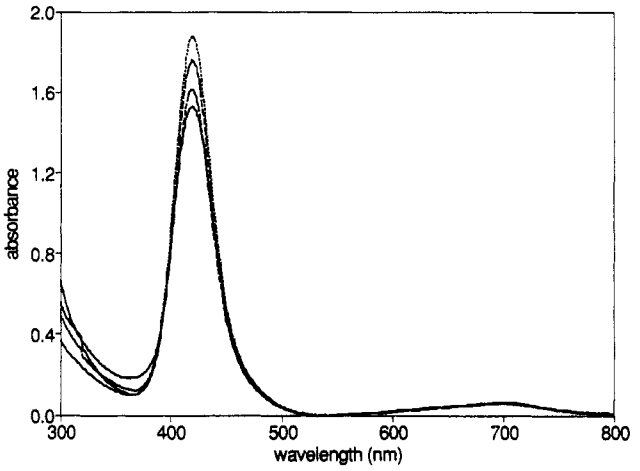

Figure 4. Visible spectra of several different samples of green "$[LWOCl_2]PF_6$" in acetonitrile showing variable A_{419}/A_{695} relative intensity.

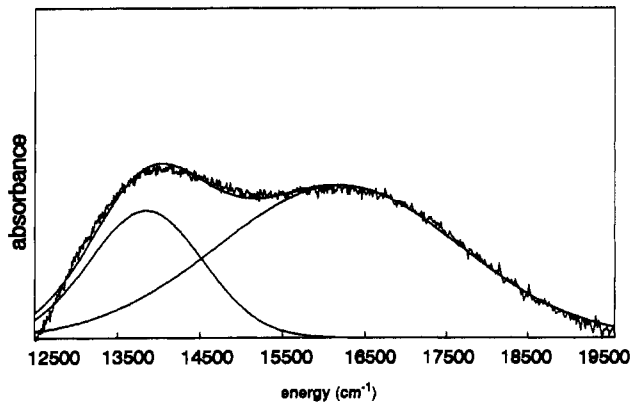

Figure 5. Deconvoluted visible spectrum of blue $[LWOCl_2]PF_6$ in acetonitrile. The peak at 13 850 cm^{-1} has ϵ = 18 L mol^{-1} cm^{-1}; the peak at 16 190 cm^{-1} has ϵ = 15 L mol^{-1} cm^{-1}.

the same instrument under the same experimental conditions. The room-temperature isotropic EPR spectra originally reported for the blue and green forms also showed nearly identical $\langle g \rangle$ values (blue, 1.775; green, 1.790).[2a] EPR spectroscopy was used to follow the progress of reaction 1 by periodically transferring aliquots of the reaction solution to quartz EPR tubes and then quenching the reaction by freezing the sample in liquid nitrogen. The resulting glasses were of excellent quality. Early in the progress of reaction 1 two different paramagnetic complexes were present, as evidenced by small spectral changes in the region g = 1.80–1.73. The major species was $[LWOCl_2]^+$, the final paramagnetic product. The minor paramagnetic species slowly decreased in concentration as the concentration of $[LWOCl_2]^+$ increased.

UV–visible electronic spectra of the blue and green materials are similar to those reported previously for these materials[2a] (Figures 4 and 5). For the present green form, however, the ratio of the absorbance of the peak at 419 nm to that of the peak at 695 nm varies with preparation (Figure 4), indicting that the green form is a mixture of at least two different materials whose relative concentrations differ among preparations. Similar behavior was observed for visible spectra of green "$LTiCl_3$", which later was characterized to be a mixture of pure $LTiCl_3$ (blue) and $LTiOCl_2$ (yellow).[15]

The original visible spectroscopic study of the blue $[LWOCl_2]PF_6$ reported a single broad peak with a λ_{max} of 715 nm.[2a] The present data confirm this broad peak but also show a second maximum at 610 nm. These broad peaks were deconvoluted using a Gaussian fitting program[22] (Figure 5). The splitting of the d → d band is ascribed to spin–orbit coupling and to ligand

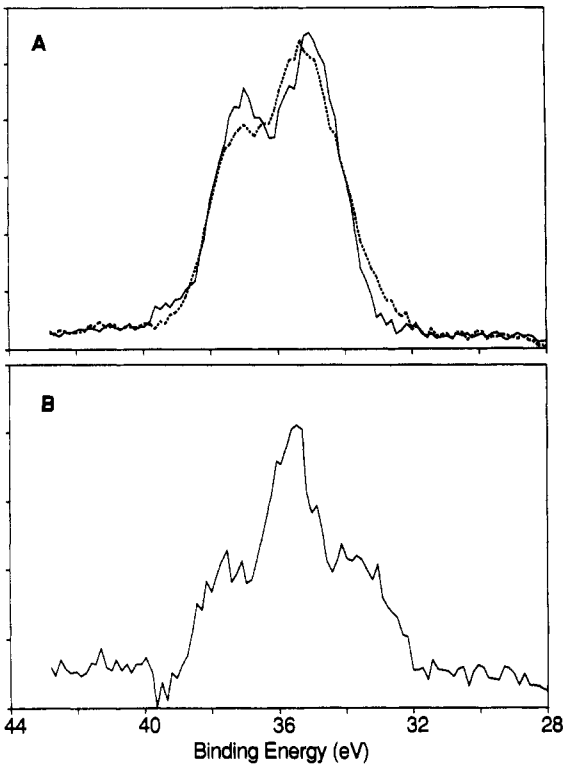

Figure 6. XPS spectra of blue $[LWOCl_2]PF_6$ and the 7-day green preparation: (A) blue (—) and green (···); (B) green − (0.70)blue.

field splitting of the $\{d_{xz}, d_{yz}\}$ LUMO of the d^1 $[LWOCl_2]^+$ cation. The peak-to-peak energy separation of 2340 cm^{-1} is similar to the magnitude of the spin–orbit interaction expected for tungsten(V) (≈2700 cm^{-1} for the free ion).[23] The nondegeneracy of the d_{xz} and d_{yz} orbitals is also supported by the rhombic EPR spectrum of blue $[LWOCl_2]PF_6$ in frozen solution (Figure 3). The relative intensity of the two bands in the visible spectrum of blue $[LWOCl_2]PF_6$ is invariant for different preparations of the compound.

X-ray photoelectron spectroscopy of core electron binding energies is a powerful method for investigating the oxidation states of metal atoms in solids.[9,24,25] For tungsten, the binding energy of the tungsten 4f electrons shifts approximately 0.9 eV toward higher binding energy with each unit increase in formal oxidation state.[26] In addition, the characteristic pattern of the $4f_{5/2}/4f_{7/2}$ spin–orbit splitting for tungsten provides a good criterion for the homogeneity of the tungsten oxidation states within the solid.

The XPS spectrum of blue $[LWOCl_2]^+$ is representative of that expected for the tungsten 4f region of a tungsten(V) species (Figures 6A and 7A), showing a well-defined $4f_{5/2}/4f_{7/2}$ peak separation. Both the 7-day (Figure 6A) and 2-day (Figure 7A) green preparations show broad poorly resolved XPS peaks, whose overall shapes and apparent binding energies are significantly different for the two green preparations.

Difference XPS was previously used to demonstrate that the green form of *cis,mer*-$MoOCl_2(PMe_2Ph)_3$ was actually a mixture and not a distortional isomer.[9] For the present study, the

(22) Chandramouli, G. V. R.; Lalitha, S.; Manoharan, P. T. *Comput. Chem.* **1990**, *14*, 257.
(23) Figgis, B. N. *Introduction to Ligand Fields*; Wiley Interscience: New York, 1966.
(24) (a) Feltham, R. D.; Brant, P. *J. Am. Chem. Soc.* **1982**, *104*, 641. (b) Brant, P.; Feltham, R. D. *Inorg. Chem.* **1980**, *19*, 2673.
(25) Salmon, D. J.; Walton, R. A. *Inorg. Chem.* **1978**, *17*, 2379. Careful analysis of the osmium 4f XPS spectrum of "$OsOCl_3(PPh_3)$" prompted a reformulation of this formally Os(V) species as an intimate mixture of $Os^{VI}O_2Cl_2(PPh_3)_2$ and $Os^{IV}Cl_4(PPh_3)_2$.
(26) Wagner, C. D.; Riggs, W. M., Davis, L. E., Moulder, J. F., Mullenburg, G. E., Eds. *Handbook of Photoelectron Spectroscopy*; Perkin Elmer Corp.: Eden Prairie, MN, 1979.

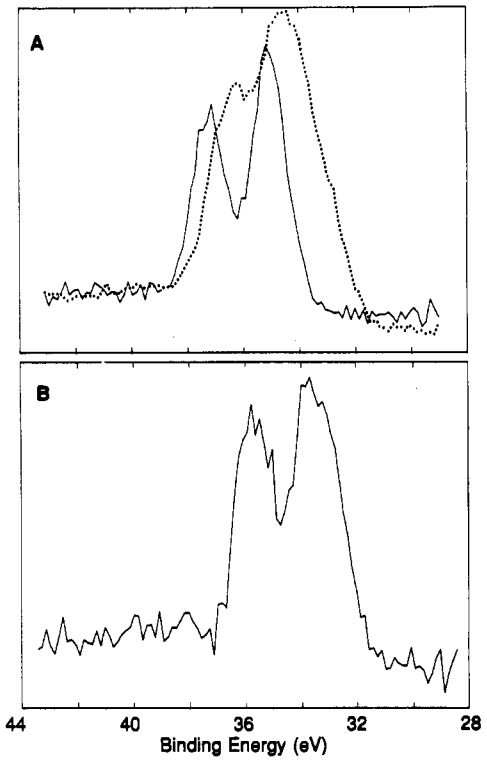

Figure 7. XPX spectra of blue $[LWOCl_2]PF_6$ and the 2-day green preparation: (A) blue (—) and green (···); (B) green − (0.50)blue.

Table 1. Mole Fractions of Tungsten Oxidation States in Green Preparations As Estimated by XPS

	W(IV)	W(V)	W(VI)
2-day green	0.35	0.60	0.05
7-day green	0.12	0.70	0.18

difference spectrum obtained by subtraction of the XP spectrum of pure blue $[LWOCl_2]PF_6$ from the XPS data for the green materials is dependent upon the green preparation. The difference spectrum resulting from the 7-day green preparation shows three broad peaks in a roughly 1:2:1 ratio (Figure 6B), rather than a distinct $^5/_2$,$^7/_2$ doublet. This result is inconsistent with a simple two-component mixture and implies that at least three different tungsten oxidation states must be present. The difference spectrum for the 7-day green preparation can be satisfactorily reproduced by assuming that the central peak is the summation of the $4f_{5/2}$ peak of tungsten(IV) and the $4f_{7/2}$ peak of tungsten(VI) components in a 40:60 ratio, respectively. A nearly identifical difference spectrum was also obtained from the XPS data collected in 1985 for an original sample of the green tungsten material. Even then, at least one individual suggested that the XPS data indicated that green form was not a pure homogeneous material.[27]

The difference spectrum for the 2-day green preparation (Figure 7B) has the appearance of a somewhat broadened tungsten(IV) 4f spectrum, consistent with the presence of a greater fraction of tungsten(IV) in the mixture. However, the $4f_{5/2}$ peak of the difference spectrum appears to be more intense than expected for a pure tungsten(IV) spectrum, presumably due to the contribution of a small amount of the $4f_{7/2}$ component of the tungsten(VI) fraction. Table 1 summarizes the compositions of the two different green preparations as determined from the XPS data.

Cyclic Voltammetry. The present voltammogram of blue $[LWOCl_2]PF_6$ is identical to the one originally reported for this material.[2b] However, the cyclic voltammograms (CV's) for the green materials vary with preparation and solvent. The 2-day green product shows three waves (Figure 8 and Table 2). In DMF the more positive reduction potential (−1.14 vs ferrocene/ferrocenium) corresponds to that observed for the pure blue species and for the major component originally reported as the green form.[2b] This wave can be confidently assigned to reversible one-electron reduction of the $[LW^{V}OCl_2]^+$ ion. The reduction potential of the middle peak (−1.43 V) is identical to that of the minor species detected in the original CV that was assigned to the reversible one-electron reduction of the $[LW^{VI}O_2Cl]^+$ ion.[2b] The most negative wave in the CV of the 2-day green form (−1.61 V) was not previously observed; this wave is assigned to the redox chemistry of an oxo–W(IV) species, possibly the $[LW^{IV}OCl(sol)]^+/[LW^{V}OCl(sol)]^{2+}$ couple (sol = solvent). Similar electrochemical behavior has been observed for related molybdenum species.[28]

(27) Nebesny, K. Private communication.

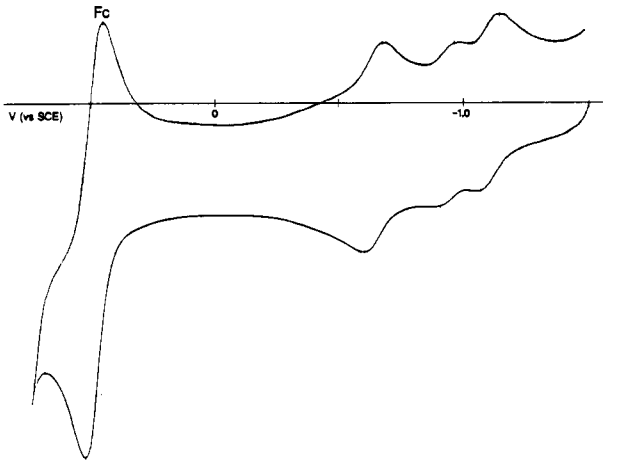

Figure 8. Cyclic voltammogram of 2-day green "$[LWOCl_2]PF_6$" in DMF. Fc is the ferrocene/ferrocenium internal standard.

Table 2. Half-Cell Potentials in Several Solvents

	solvent	$E_{1/2}$ (V)[a]		
blue	DMF	−1.14		
2-day green	DMF	−1.14	−1.43	−1.61
	acetonitrile	−1.08	−1.38	−1.57
	pyridine	−1.16		−1.61
7-day green	DMF	−1.10	−1.44	
	acetonitrile	−1.05	−1.36	
	pyridine	−1.08	−1.43	

[a] All potentials relative to $E_{1/2}$ of the Fc/Fc^+ couple as internal standard.

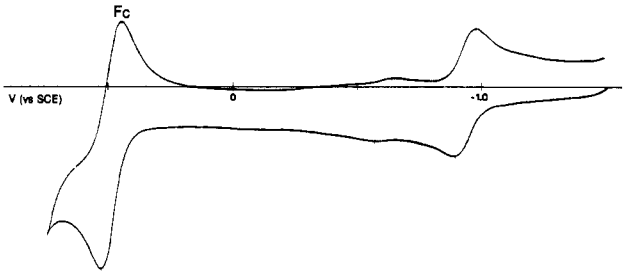

Figure 9. Cyclic voltammogram of 7-day green "$[LWOCl_2]PF_6$" in DMF. Fc is the ferrocene/ferrocenium internal standard.

The 7-day green product shows two waves in all of its CV's, and the more negative wave (−1.44 V) has the greater relative intensity (Figure 9). This wave is likely due to the reduction of a $[LW^{VI}O_2Cl]^+$-like species (*vide supra*) or to the reduction of the dimeric $[L_2W^{VI}_2O_5]^{2+}$ ion (−1.43 V) formed by hydrolysis of $[LW^{VI}O_2Cl]^+$.[2b] The minor peak in the 7-day CV (−1.10 V) is

(28) The related $L'Mo^{IV}OCl(sol)$ complexes (L' = hydrotris(3,5-dimethyl-1-pyrazolyl)borate) are known to undergo reversible one-electron oxidation at potentials more negative than those of the $L'Mo^{V}OCl_2^{0/-}$ and $L'Mo^{VI}O_2Cl^{0/-}$ couples: LaBarre, M. J. Ph.D. Dissertation, University of Arizona, 1992.

assigned to reduction of the $[LW^{V}OCl_2]^+$ ion. No distinct wave at −1.6 V is observed in the 7-day green material.

The CV's for the green materials indicate that as many as three tungsten species can be present in solution. The relative amount of each species observed in a given CV depends upon the initial reaction time, the solvent, and the scan rate (Table II). These CV results suggest that competitive solvent-dependent chemical processes occur among the various tungsten species in solution (*vide infra*).

Quantitative comparisons between the CV and XPS experiments of the green materials are not possible because of the demonstrated solvent dependence of the CV measurements. However, the electrochemical measurements and the XPS results are both qualitatively consistent with the idea that the green materials are mixtures of at least three components. The relative amounts of these components in the isolated green solid vary with the time of reaction 1. The XPS data for the 7-day green preparation show the mole fraction of W(V) > W(VI) > W(IV), whereas the 2-day preparation shows the mole fraction of W(V) > W(IV) > W(VI). The CV's of the green preparations are qualitatively consistent with the XPS results. The absolute magnitudes of the waves in the CV's vary with solvent, but their relative magnitudes are conserved. For example, the most negative wave of the 2-day green preparation (assigned to the $[LW^{IV}OCl(sol)]^+/[LW^{V}OCl(sol)]^{2+}$ couple) is more intense than the center wave (assigned to the one-electron reduction of a tungsten(VI) species (*vide supra*)); XPS analysis also indicated more tungsten(IV) than tungsten(VI) for this sample.

Infrared spectra of the blue and green materials are complicated in the 1000–900-cm^{-1} region where $\nu(W{=}O)$ bands are expected to appear because strong ligand absorptions also occur in this region. The original report assigned vibrations at 980 cm^{-1} (blue form) and 960 cm^{-1} (green form) to $\nu(W{=}O)$.[2] For the present blue $[LWOCl_2]PF_6$ sample, the most intense peak in the 1000–900-cm^{-1} region occurs at 978 cm^{-1}. In $LW(CO)_3$, which has no oxo groups, a ligand peak occurs at nearly the same frequency. However, in $LW(CO)_3$, this ligand peak exhibits approximately half the intensity of the adjacent ligand vibration at 995 cm^{-1}. Least-squares fitting of the infrared absorpion spectrum of blue $[LWOCl_2]PF_6$ assuming Gaussian peak shapes (Figure 10A) shows two overlapping strong peaks at 977 and 981 cm^{-1}. Definitive confirmation of the assignment of $\nu(W{=}O)$ for blue $[LWOCl_2]PF_6$ was made by ^{18}O substitution. The spectrum of the ^{18}O-labeled complex shows a decrease in the relative intensity of the 981-cm^{-1} component (Figure 10B) and a new intense peak at 924 cm^{-1} due to $\nu(W{=}^{18}O)$. The least-squares fittings of Figure 10 also indicate that the low-symmetry $[LWOCl_2]^+$ ion has additional ligand vibrations at 964, 969, 993, and 998 cm^{-1} that are substantially weaker than the ligand band at 977 cm^{-1}.

The IR spectra of the green materials in the 1000–900-cm^{-1} region vary among preparations (Figure 11). The major differences occur in the peaks near 920, 960, and 980 cm^{-1}. The 2-day green material shows a very weak band at 919 cm^{-1} and a peak of medium intensity at 967 cm^{-1}; the strongest peak in this region for the 2-day green material occurs at 982 cm^{-1}. For the 7-day green material, the strongest peak occurs at 923 cm^{-1}; a peak at 960 cm^{-1} is of intensity comparable to that of a group of overlapping peaks at 972, 978, and 985 cm^{-1}. A pair of peaks, with the lower energy peak being more intense, is the infrared signature of a *cis*-MO_2^{2+} moiety (M = Mo,[37] W[32]). Thus, the increase in intensity of the peaks at 923 and 960 cm^{-1} with increasing reaction time is consistent with the formation of a *cis*-WO_2^{2+} component. The original spectrum of green "$[LWOCl_2]PF_6$",[38] as well as a recent spectrum of the original material, also shows peaks near 920, 960, and 980 cm^{-1}. These vibrations can be assigned to the $\nu(W{=}O)$ frequencies of a mixture of blue $[LWOCl_2]PF_6$ and a *cis*-WO_2^{2+} component. There is no need to invoke the concept of distortional isomerism to explain the band at 960 cm^{-1} in the green preparations.

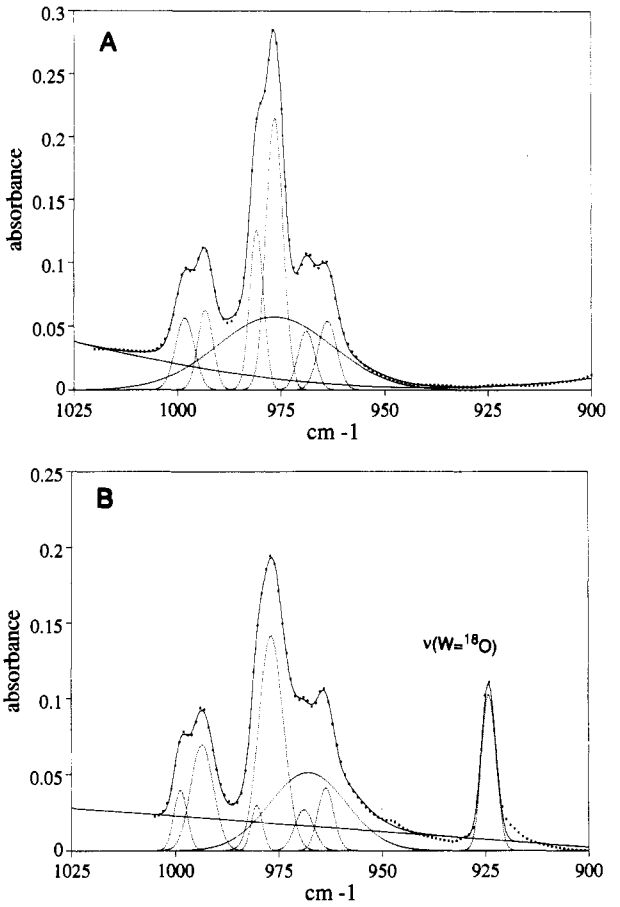

Figure 10. Least-squares fit of the infrared absorption spectra of blue $[LWOCl_2]PF_6$ (A) and $[LW^{18}OCl_2]PF_6$ (B). The squares are the digitized data (1 point/cm^{-1}); the dashed lines are the individual Gaussian components; the solid line is the sum of the Gaussian components and the baseline absorbance.

Raman Spectroscopy. Blue $[LWOCl_2]PF_6$ shows a very strong asymmetric peak with a maximum at 974 cm^{-1}. Labeling with ^{18}O produces a new peak at 925 cm^{-1}. The 2-day green material has a peak at 964 cm^{-1} that is much more intense than the strong ligand bands and that is assigned to $\nu(W{=}O)$ for the postulated oxo–W(IV) species (Figure 12B). The 7-day green material (Figure 12A) shows the strong peak at 964 cm^{-1} plus a new medium-intensity peak at 920 cm^{-1} and a new strong peak at 957 cm^{-1}. The latter two frequencies are nearly identical to those observed in the IR of the 7-day green material (Figure 11B), but their relative intensities are reversed. By analogy with previous studies of MoO_2^{2+} complexes,[29] the Raman bands at 920 and 957 cm^{-1} can be assigned to the antisymmetric and symmetric stretches, respectively, of a *cis*-WO_2^{2+} group. Thus, the Raman spectra of the green materials also point to their being a mixture of oxo–W(IV,V,VI) species whose composition depends upon the time of reaction 1.

X-ray Crystallography and Crystal Chemistry. The chromatographic and spectroscopic data presented above indicate that blue $[LWOCl_2]PF_6$ is a pure homogeneous material. X-ray structure determinations of blue single crystals from an original sample and from the present work (supplementary material) have shown that both are isomorphous and isostructural with the crystal studied previously.[2a] The W=O distance of 1.70(1) Å is within experimental error of previously reported distance[2a] of 1.72(2) Å and within the typical range for W=O distances.[30] However, several crystallographic complications are present in the structure

(29) Willis, L. J.; Loehr, T. M. *Spectrochim. Acta* **1987**, *43A*, 51.

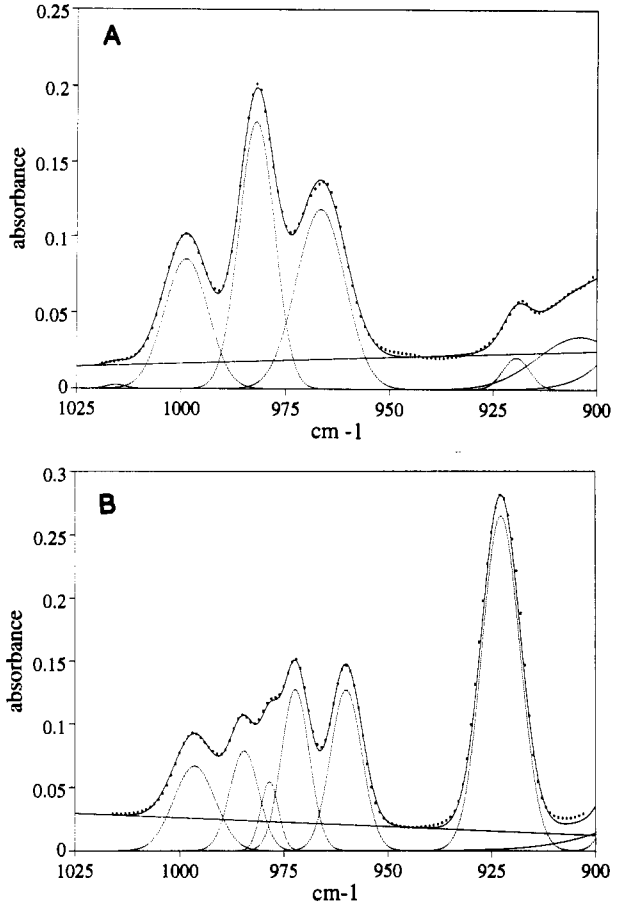

Figure 11. Least-squares fit of the infrared absorption spectra of green "$[LWOCl_2]PF_6$": (A) 2-day preparation; (B) 7-day preparation. The squares are the digitized data (1 point/cm^{-1}); the dashed lines are the individual Gaussian components; the solid line is the sum of the Gaussian components and the baseline absorbance.

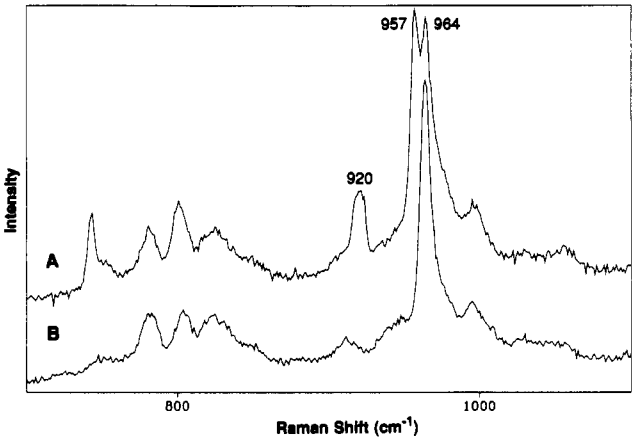

Figure 12. Raman spectra of solid green "$[LWOCl_2]PF_6$": (A) 7-day preparation; (B) 2-day preparation.

that were not readily apparent in the original communication[2a] that depicted all atoms of the $[LWOCl_2]^+$ ion as spheres and which gave no C–C distances. The carbon skeleton of the triazacyclononane ligand is conformationally disordered, as evidenced by the large anisotropic thermal parameters (Figure 13) and by the unrealistically short C–C bond lengths (1.39–1.42(3) Å). The nearly spherical PF_6^- ion exhibits complex rotational disorder. In addition, several weak reflections violate the extinction conditions of the glide planes for space group *Pbcm*. These crystallographic complications are also present in the

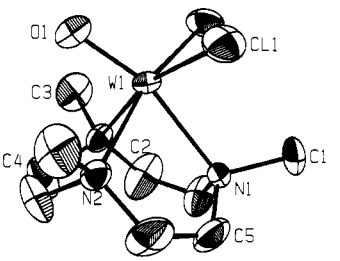

Figure 13. Perspective view of the structure of the blue $[LWOCl_2]^+$ ion after anisotropic refinement. The crystallographically imposed mirror plane is approximately in the plane of the paper.

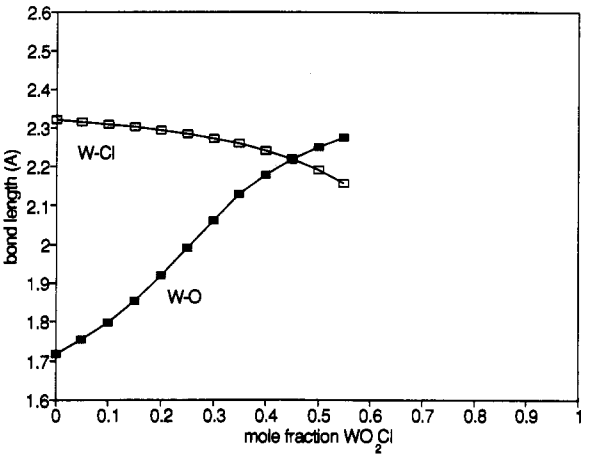

Figure 14. Apparent W–O and W–Cl lengths in $WOCl_2$ with increasing mole fraction of $W(O_c)_2Cl_o$, calculated from the model shown in Figure 1.

original green crystals that exhibit an unusually long W=O bond (*vide infra*).

Parkin and co-workers have clearly shown that small amounts of cocrystallized impurities are difficult or impossible to detect directly by X-ray crystallography.[7,31] However, such "compositional disorder" is often manifest as anomalous metal–ligand bond lengths. Can the unusually long W–O bond (1.89 Å) previously found for the green form of "$[LWOCl_2]PF_6$" also be explained as a crystallographic artifact due to cocrystallization of a minor species with blue $[LWOCl_2]PF_6$? Initial consideration of the precursors and possible side products formed during the synthesis of the green form[2] of $[LWOCl_2]PF_6$ suggested that the yellow species, $[LWO_2Cl]PF_6$, was the most likely compound. Infrared analysis of the green reaction mixture over time indicated an increasingly more intense pair of bands at 960 and 922 cm^{-1} characteristic of the *cis*-WO_2^{2+} unit.[2,32] Figure 1 shows that cocrystallization of $[LWO_2Cl]PF_6$ with $[LWOCl_2]PF_6$ would introduce Cl atom density near the O atom site of $[LWOCl_2]PF_6$ and thereby increase the apparent W–O bond distance. Model crystallographic calculations[21] show that an apparent W–O distance of 1.89 Å results from doping 0.15–0.20 mole fraction of yellow $[LWO_2Cl]PF_6$ into blue $[LWOCl_2]PF_6$ (Figure 14). The calculated electron density for the oxo group shows no unusual intensity or shape at this level of compositional disorder.[21]

It was previously noted that blue $[LWOCl_2]PF_6$ could be obtained when the green form was recrystallized from acetonitrile/water mixtures.[2b] On one occasion, large blue plates (10 × 5 × 1 mm) formed from a toluene/acetonitrile solution that had been allowed to evaporate to dryness undisturbed. Examination of these large blue plates under a microscope revealed the presence of small yellow domains (≤0.7 mm in maximum dimension) on

(30) Nugent, W. A.; Mayer, J. M. *Metal-Ligand Multiple Bonds*; Wiley Interscience: New York, 1988.

(31) Yoon, K.; Parkin, G. *J. Am. Chem. Soc.* **1991**, *113*, 8414.

(32) (a) Yamanouchi, K.; Yamada, S. *Inorg. Chim. Acta* **1974**, *11*, 223. (b) Brisdon, B. J. *Inorg. Chem.* **1967**, *6*, 1791. (c) Gibson, V. C.; Kee, T. P.; Shaw, A. *Polyhedron* **1988**, *7*, 579. (d) De Wet, J. F.; Caira, M. R.; Gellatly, B. J. *Acta Crystallogr.* **1978**, *B34*, 762.

Table 3. Refined Orthorhombic Unit Cells (*Pbcm*) for the Blue and Green Materials

sample	λ^a	no. of refl	$\Delta 2\theta^b$	a (Å)	b (Å)	c (Å)
blue (c)[c,d]	Mo	34		7.223(4)	14.898(6)	16.535(8)
blue (c)[e]	Mo	25		7.162(1)	14.839(3)	16.553(2)
blue (p)[e,f]	Cu	31	0.05	7.135	14.792	16.532
green (c)[d]	Mo	28		7.267(5)	14.95(1)	16.49(1)
7-day green (p)[e]	Cu	29	0.05	7.060	14.625	16.695

[a] $\lambda_{Mo} = 0.710\,73$ Å, $\lambda_{Cu} = 1.540\,60$ Å. [b] Maximum deviation between $\theta(hkl)_{calc}$ and $\theta(hkl)_{obs}$. [c] Method: (c) = single crystal; (p) = powder diffraction. [d] Data from ref 2. [e] Reference 21. [f] The refined powder cells have errors on the order of 1%.

the surface. The blue plates extinguished polarized light sharply, but the yellow domains did not. Occluded domains within the large blue plates appeared green. A few milligrams of each component were hand-separated from the material with a dissecting needle, and the IR spectrum of each sample was recorded. The IR spectrum of the blue fraction matched that of pure blue $[LWOCl_2]PF_6$; the IR spectrum of the yellow domains was similar to that of the 7-day green material. These results further support the suggestion that yellow $[LWO_2Cl]PF_6$ is a component of the green material.

All attempts to prepare pure single crystals of $[LWO_2Cl]PF_6$ were unsuccessful, presumably due to facile hydrolysis to the colorless $[L_2W_2O_5]^{2+}$ ion[2b] in the presence of trace amounts of water. Therefore, it was not possible to experimentally study mixed crystals of varying compositions as has been done for the green $MoOCl_2(PMe_2Ph)_3$ system.[7]

Reinvestigation of several green crystals from an original preparation[2] showed that they sharply extinguished polarized light. A representative octahedrally-shaped crystal diffracted X-rays strongly to $2\theta = 80°$ ($d = 0.55$ Å) and exhibited a mosaic spread of $\approx 0.3°$. This crystal held out the hope of crystallography resolving the overlapping O and Cl sites of the compositionally disordered green crystal, as had been done previously for *cis,mer*-$MoOCl_2(PMe_2Ph)_3$.[9] Not surprisingly, however, this green crystal exhibited the same crystallographic complications discussed above for pure blue $[LWOCl_2]PF_6$, and the expected subtle disorder at the O and Cl sites could not be unambiguously resolved experimentally. After anisotropic refinement of the structure as $[LWOCl_2]PF_6$, the final thermal parameters for the Cl atoms were slightly larger than those of the O atoms, and one of the major axes of the thermal ellipsoids for the O atom was not normal to the W=O bond direction (supplementary material). The apparent W–O distance of 1.88(1) Å was indistinguishable from the 1.89(2) Å distance reported previously[2a] and indicative of about 0.2 mole fraction of $[LWO_2Cl]PF_6$ in the crystal (Figure 14).

None of the 7-day or 2-day preparations of the green form of $[LWOCl_2]PF_6$ yielded diffraction-quality crystals, despite numerous attempts. Therefore, powder X-ray diffraction was used to determine the cell type and unit cell parameters for these green materials. Pure blue $[LWOC_2]PF_6$ was used as a standard for the indexing procedure; 13 reflections common to both the single crystal and powder data were used for initial indexing of the powder data. Subsequent refinement of 31 reflections yielded a cell for the blue powder that was in complete agreement with that determined from a single crystal of the compound (Table 3). For the green powder, the initial orthorhombic unit cell (*Pbcm*) of $a = 7$, $b = 14$, and $c = 16$ Å was assumed. This initial guess produced a successful refinement of the cell parameters for the green powder from the 7-day preparation. The resultant cell was isomorphous with that for the blue solid and with those originally reported for the blue and green forms of $[LWOCl_2]PF_6$. However, it should be noted that the relative intensities of equivalent reflections of the blue and green powders were very different, which suggests that the locations of one or more atoms are somewhat different in the unit cells of the two forms. Also the reflections of the green form were found to be 3–4 times broader than those of the blue form, indicating that long-range order is correspondingly less in the green form.

The powder diffraction pattern of a sample of the 2-day green preparation exhibited several lower order reflections that were not present in the patterns of either the blue powder or the 7-day green preparation. Other physical methods of characterization (*vide supra*) have illustrated the variable composition of the 2-day and 7-day green preparations, so the observed differences in the powder diffraction patterns for these two preparations are not unexpected.

Dynamic Equilibria in Green "$[LWOCl_2]PF_6$"

The physical and spectroscopic studies described above clearly show that the green product of reaction 1 is *not* a distortional isomer as originally proposed, but rather a ternary mixture of blue $[LWOCl_2]PF_6$ (which can be independently synthesized in pure form from $[LWCl_3]Cl$ and H_2O), a dioxo–tungsten(VI) complex (most likely $[LWO_2Cl]PF_6$), and a tungsten(IV) species.

The chromatographic behavior of the crude green product of reaction 1 appears paradoxical at first glance. Passage through an acidic alumina column produces pure blue $[LWOCl_2]PF_6$ and a visibly separated apparently homogeneous trailing yellow-green band. Isolation and spectroscopic characterization of this trailing band show that it is primarily blue $[LWOCl_2]PF_6$ (up to 0.7 mole fraction). However, re-elution of this green material under identical conditions using a freshly prepared chromatographic column from the same source results in *no* further separation of the blue component from the green mixture.

We propose that reaction 1 produces three cationic oxo–tungsten complexes of similar sizes (blue $[LW^{V}OCl_2]^+$, yellow $[LW^{VI}O_2Cl]^+$, and $[LW^{IV}OCl(sol)]^+$) that are involved in two kinds of competing equilibrium processes. One process is chromatographic separation. Blue $[LWOCl_2]PF_6$ interacts with the acidic alumina less strongly than the other components and passes through the column first. However, if this were the only equilibrium process involving blue $[LWOCl_2]PF_6$, then it would be expected that further chromatography on the green eluent should separate additional pure blue $[LWOCl_2]PF_6$ from the mixture. Such is not the case. The green mixture that is eluted from the column cannot be futher separated by additional chromatography under the same conditions. This behavior of the chromatographed green mixture is consistent with a second competing equilibrium that completely scrambles the tungsten atom oxidation states through a series of atom-transfer reactions, as shown in Scheme 1.

Dissociation of solvent from the postulated $[LW^{IV}OCl(sol)]^+$ species according to equilibrium 1 would generate the five-coordinate species $[LW^{IV}OCl]^+$ that could catalyze the interconversion of W(V) and W(IV) by the chlorine atom transfer reaction of equilibrium 2; $[LW^{IV}OCl]^+$ could also catalyze the interconversion of W(VI) and W(IV) by the oxygen atom transfer reaction of equilibrium 3. Equilibria 2 and 3 are both known processes in the oxo chemistry of group 6 transition metals.[33-36] When large amounts of blue $[LW^{V}OCl_2]^+$ are present, as in the crude reaction mixture, some of this most rapidly moving cation separates from the mixture faster than it is scrambled by the atom-transfer reactions of Scheme 1. However, at lower concentrations of blue $[LW^{V}OCl_2]^+$, the scrambling reactions

(33) Harlan, E. W.; Berg, J. M.; Holm, R. H. *J. Am. Chem. Soc.* **1986**, *108*, 6992.
(34) Chen, G. J.-J.; McDonald, J. W.; Newton, W. E. *Inorg. Chem.* **1976**, *15*, 2612.
(35) Matsuda, T.; Tanaka, K.; Tanaka, T. *Inorg. Chem.* **1979**, *18*, 454.
(36) Over, D. E.; Critchlow, S. C.; Mayer, J. M. *Inorg. Chem.* **1992**, *31*, 4643.
(37) Stiefel, E. I. *Compr. Coord. Chem.* **1987**, *3*, 1375.
(38) Backes-Dahmann, G. Ph.D. Dissertation, Ruhr-Universität, Bochum, Germany, 1985.

Scheme I

EQUILIBRIUM 1

$$[LW^{IV}OCl(NCMe)]^+ \rightleftharpoons [LW^{IV}OCl]^+ + NCMe$$

EQUILIBRIUM 2

$$[LW^{IV}OCl]^+ + \underset{\text{blue}}{[LW^{V}(^{18}O)Cl_2]^+} \rightleftharpoons \left[\begin{matrix} O & & {}^{18}O \\ \| & & \| \\ LW & -Cl- & WL \\ | & & | \\ Cl & & Cl \end{matrix}\right]^{+2} \rightleftharpoons \underset{\text{blue}}{[LW^{V}OCl_2]^+} + [LW^{IV}(^{18}O)Cl]^+$$

EQUILIBRIUM 3

$$[LW^{IV}(^{18}O)Cl]^+ + [LW^{VI}O_2Cl]^+ \rightleftharpoons \left[\begin{matrix} {}^{18}O & & O \\ \| & & \| \\ LW & -O- & WL \\ | & & | \\ Cl & & Cl \end{matrix}\right]^{+2} \rightleftharpoons [LW^{VI}(^{18}O)(O)Cl]^+ + [LW^{IV}OCl]^+$$

Table 4. Estimated[a] Mole Fractions of Oxo–Tungsten Species after Statistical Scrambling of ^{18}O Atoms via Scheme 1

W–oxo species	before scrambling	after scrambling
$LW^{V}OCl_2^+$	0.257	0.365
$LW^{V}(^{18}O)Cl_2^+$	0.572	0.463
$LW^{IV}O$[b]	0.150	0.066
$LW^{IV}(^{18}O)$[b]	0	0.084
$LW^{VI}O_2$[b]	0.021	0.004
$LW^{VI}(O)(^{18}O)$[b]	0	0.011
$LW^{VI}(^{18}O)_2$[b]	0	0.007

[a] Mole fractions of species in green material from XPS; 4 mg of blue $[LW(^{18}O)Cl_2]PF_6$ + 3 mg of 2-day green; mol wt of all tungsten species = 580 (estd). [b] Exact formulation uncertain; nature of the oxo–tungsten fragment indicated.

compete with chromatographic separation, and the green mixture behaves as a homogeneous material when rechromatographed.

The similarity of the colors of the green solid and the green solutions suggests that very little of the W(V)–O–W(V) dimer is present in solution. To test this hypothesis, the absorbance of the 419-nm band in a sample of the 2-day green preparation was measured over a wide range of relative concentrations. The net result was a strict adherence of the data to Beer's law, which implies that any equilibrium between the W(IV) and W(VI) monomers and a W(V)–O–W(V) dimer lies well toward the side of the monomers in this case.

Scheme 1 implies that an ^{18}O label will become statistically distributed among the oxo–tungsten(IV,V,VI) complexes proposed to be present. To test further the proposed equilibria, a mixture of the chromatographed 2-day green preparation and pure blue $[LWOCl_2]PF_6$ (ca. 95% ^{18}O labeled) was dissolved in acetonitrile, and the solution was stirred for several hours. Periodically a few drops of the solution were removed and placed on a NaCl plate, and the acetonitrile was allowed to evaporate. The infrared spectrum of the residue was recorded over the range 1100–700 cm^{-1}. Table 4 shows the expected mole fractions of the various $W(^{18}O)$ species before and after statistical scrambling of the ^{18}O atoms among the postulated oxo–tungsten complexes. Figure 15 shows the results of the scrambling experiment. The new band at 916 cm^{-1} can be explained by the generation of a $W^{IV}{=}{}^{18}O$ species by equilibrium 2 of Scheme 1 and the mass effect on the postulated monooxo–W^{IV} species observed in the Raman spectrum (Figure 12A) [(0.948)(964 cm^{-1}) = 914 cm^{-1}]. The frequency shifts of a *cis*-MO_2 unit upon ^{18}O substitution are complex due to the strong coupling between the symmetric and antisymmetric stretching vibrations.[29] By analogy to previous studies of isotopically labeled six-coordinate *cis*-$Mo^{VI}O_2$ complexes,[29] the new peak at 904 cm^{-1} is assigned to the isotopically shifted symmetric stretch of a doubly labeled *cis*-$W^{VI}(^{18}O)_2$ unit.

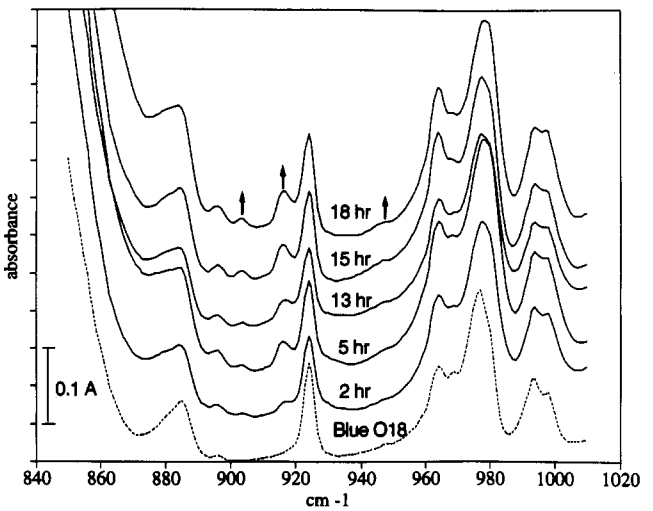

Figure 15. Infrared absorption spectra of a mixture of blue $[LW(^{18}O)Cl_2]PF_6$ and 2-day green material as a function of reaction time in acetonitrile at room temperature. The spectra are normalized to the intense PF_6^- band at 840 cm^{-1}. The dotted trace shows the spectrum of blue $[LW^{18}OCl_2]PF_6$; successive offset solid lines show the spectra of the mixture. The arrows show the new $W{=}{}^{18}O$ vibrations that grow in from the equilibria of Scheme 1.

The low intensity of this band is consistent with the small amount (ca. 0.05 mole fraction) of *cis*-WO_2^{2+} present in the 2-day green preparation and with the amount of $[LW^{18}OCl_2]PF_6$ added in the experiment. The frequency shift for the monosubstituted *cis*-$W(^{16}O)(^{18}O)$ unit is expected to be about 10–20 cm^{-1} from comparison to the *cis*-MoO_2 complexes and may be split by solid-state site symmetry effects. The weak broad shoulder that appears at about 950 cm^{-1} is assigned to the monosubstituted species. The strong antisymmetric stretch of the *cis*-WO_2^{2+} group is predicted to shift to the 870-cm^{-1} region upon ^{18}O labeling and is obscured by the intense broad absorbance of the PF_6^- ion. Thus, the results of the scrambling experiment are completely consistent with facile atom-transfer reactions among oxo–W(IV,V,VI) species as shown in Scheme 1.

Conclusions

The chemical and spectroscopic results presented above provide compelling evidence that the green form of $[LWOCl_2]PF_6$ is *not* a distortional (bond stretch) isomer of blue $[LWOCl_2]PF_6$. Rather, the green form is actually a complicated ternary mixture of oxo–W(IV,V,VI) species that are in dynamic equilibrium in solution. These experimental results support the conclusion from recent *ab initio* theoretical studies that distortional (bond stretch)

isomerism is not energetically feasible for the $[LWOCl_2]^+$ system.[8]

We wish to reemphasize here that *cocrystallization* of molecules of similar size and charge distribution can minimize the free energy of crystallization (ΔG_{cryst}) due to the increased entropy of the mixed crystal:[9]

$$\Delta G_{cryst} = \Delta H_{cryst} - T\Delta S_{cryst}$$

Doping a paramagnetic species into a diamagnetic single crystal host lattice is a standard technique in EPR spectroscopy, but the effects of mixed crystals upon conventional X-ray structure determinations of transition-metal complexes had been largely ignored prior to 1991. Parkin *et al.* have elegantly demonstrated that it is often impossible to directly detect that a crystal is a mixture by X-ray crystallography.[31] However, the final metal–ligand bond lengths derived from mixed crystals are frequently anomalous when compared to those of similar compounds in crystallographic data bases. Such anomalies are one indication that the crystal may be a mixture and that additional experimental work is needed.

Sorting out the exact nature of a mixture can be a difficult and tedious process, as illustrated by the present study. Chromatography and a broad range of spectroscopic studies on different preparations can provide additional evidence for a mixture, but dynamic equilibria among the components, as found in the present study, may thwart separation. Synthesis of the presumed individual components is the ideal way to firmly establish the nature of a mixture. However, it may not be possible to prepare each compound in pure form, or one or more of the components may be a presently unknown compound.

Finally, we note that any other claims of bond stretch isomers in coordination compounds[11] must be judged solely on their own merits because both of the highly cited precedents, green *cis,mer*-$MoOCl(PMe_2Ph)_3$[3,4] and green $[LWOCl_2]PF_6$,[2] have been shown to be mixtures.

Acknowledgment. Partial support of this research by a grant from the National Institutes of Health (GM-37773), a NATO Research Grant (86/0513), and the Materials Characterization Program of the University of Arizona is gratefully acknowledged. J.H.E. thanks the Alexander von Humboldt Foundation for a Senior Scientist Award. We thank Dr. A. Raitsimring for assistance with the EPR spectra, Dr. T. M. Loehr for the use of his laser Raman facilities and for helpful discussions, Dr. L. Subramanian for her assistance with Gaussian fitting of the blue visible spectrum, Dr. S. A. Roberts for helpful discussion, and Ms. Zheng Li for assistance with the X-ray crystallography.

Supplementary Material Available: ORTEP views and tables of crystal data, positional parameters, displacement coefficients, bond distances and angles, and infrared data for the blue and green materials (9 pages). Ordering information is given on any current masthead page.